JOURNAL OF GUIDANCE, CONTROL, AND DYNAMICS
Vol. 24, No. 2, March–April 2001

Robust Autopilot for a Quasi-Linear Parameter-Varying Missile Model

Antonios Tsourdos, Rafał Żbikowski, and Brian A. White
Cranfield University, Swindon, England SN6 8LA, United Kingdom

A sideslip velocity autopilot is designed for a model of a tactical missile, and robust stability of the closed-loop system is investigated. The tail-controlled missile in the cruciform fin configuration is modeled as a second-order quasi-linear parameter-varying system. This nonlinear model is obtained from the Taylor linearized model of the horizontal motion by including explicit dependence of the aerodynamic derivatives on a state (sideslip velocity) and external parameters (longitudinal velocity and roll angle). The autopilot design is based on input–output pseudolinearization, which is the restriction of input–output feedback linearization to the set of equilibria of the nonlinear model. The design makes Taylor linearization of the closed-loop system independent of the choice of equilibria. Thus, if the operating points are in the vicinity of the equilibria, then only one linear model will describe closed-loop dynamics, regardless of the rate of change of the operating points. Simulations for constant lateral acceleration demands show good tracking with fast response time. Parametric and H_∞ stability margins for uncertainty in the controller parameters and aerodynamic derivatives are analysed using Kharitonov's approach. The analysis shows that the design is fairly robust with respect to both kinds of uncertainty.

I. Introduction

ONE of the most popular methods for applying linear time-invariant (LTI) control theory to time-varying and/or nonlinear systems is gain scheduling.[1] This strategy involves obtaining Taylor linearized models for the plant at finitely many equilibria (set points), designing an LTI control law (point design) to satisfy local performance objectives for each point, and then adjusting (scheduling) the controller gains in real time as the operating conditions vary. This approach has been applied in practice, particularly for aircraft.

An early theoretical investigation into the performance of parameter-varying systems can be found in Ref. 2. During the 1980s, Rugh,[1] Baumann and Rugh,[3] and Wang and Rugh[4] developed an analytical framework for gain scheduling using extended linearization. Also, Shamma and Athans[5–7] introduced linear parameter-varying (LPV) systems as a tool for quantifying such heuristic design rules as

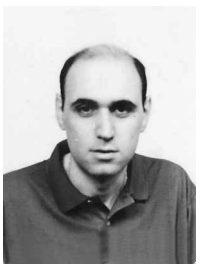

Antonios Tsourdos was born in Crete, Greece in 1969. He received his B.S. in electronic, control, and systems engineering from the University of Sheffield in 1995, his M.S. in systems engineering from the University of Wales, Cardiff in 1996, and a Ph.D. from Cranfield University, Royal Military College of Science (RMCS) in 1999. He is currently a lecturer in the Department of Aerospace, Power, and Sensors, Cranfield University, RMCS. His doctoral dissertation was in robust control of an autopilot for a high-incidence nonlinear missile with uncertain parameters. His research interests include robust and nonlinear control design, missile guidance, and control of linear parameter-varying systems; tsourdos@rmcs.cranfield.ac.uk.

Rafał Żbikowski is a Senior Officer in the Guidance and Control Group of the Department of Aerospace, Power, and Sensors at Cranfield University's Shrivenham campus (Royal Military College of Science). Prior to this he was a Postdoctoral Research Fellow at Glasgow University leading the Glasgow side of a joint project with Daimler–Benz on neural adaptive control technology. Rafał Żbikowski completed his M.S. (Special Honors) in robust adaptive control at Warsaw University of Technology, Poland in 1990 and received a Ph.D. in neural adaptive control from Glasgow University, Scotland, in 1994. He has published over 30 papers (including 7 journal papers), mostly on adaptive and nonlinear aspects of intelligent control. He is a regular reviewer for several professional journals and a member of the American Mathematical Society (AMS) and the Institute of Electrical and Electronics Engineers (IEEE). His current research focuses on missile guidance and control and flapping wing autonomous micro air vehicles; zbikowsk@rmcs.cranfield.ac.uk.

Brian A. White gained his B.S. in engineering from the University of Leicester in 1968 and his M.S. in the theory and practice of control engineering from UMIST in 1972. He studied for his Ph.D. at the University of Manchester Institute of Science and Technology in 1974. He worked for British Aerospace at Filton designing guided weapon systems from 1968 to 1971 and was instrumental in introducing Kalman filtering into guidance systems. He became a lecturer at Bath University in the school of Electrical Engineering from 1974 to 1986 and is now head of the Department of Aerospace, Power, and Sensors in the Faculty of Defense Technology at Cranfield University. His areas of expertise are robust control; nonlinear control, estimation, and observer applications; inertial navigation; guidance design; soft computing; and sensor and data fusion; brian@rmcs.cranfield.ac.uk.

Received 19 August 1999; revision received 10 April 2000; accepted for publication 11 April 2000.

the resulting parameter must vary slowly and the scheduling parameter must capture the nonlinearities of the plant. Shahruz and Behtash[8] suggested using LPV systems for synthesising gain-scheduled controllers, and Shamma and Cloutier[9] have used LPV plant models for designing missile autopilots.

Attention has since turned to performance and design of parameter-dependent controllers for LPV systems. Performance is usually measured in terms of the induced L_2 norm, and controllers are designed for certain classes of parameter variations, for example, real or complex values, arbitrarily fast or bounded rates of variation, shape of the parameter envelope, etc. The resulting parameter-dependent controllers are scheduled automatically, so that the often arduous task of scheduling a complex multivariable controller a posteriori is avoided.

In this paper, a sideslip velocity autopilot is designed for a realistic model of a tactical missile, and robust stability of the closed-loop system is investigated.

The tail-controlled missile in the cruciform fin configuration[10] is modeled as a second-order quasi-linear parameter-varying (QLPV) system. This nonlinear model is obtained from the Taylor linearized model of the horizontal motion by including explicit dependence of the aerodynamic derivatives on a state (sideslip velocity) and external parameters (longitudinal velocity and roll angle). The first contribution is to consider this detailed QLPV (and, thus, nonlinear) model.

The autopilot design is based on input–output pseudolinearization.[11–13] The design makes Taylor linearization of the closed-loop system independent of the choice of equilibria. Thus, if the operating points are in the vicinity of the equilibria, then one and only one linear model will describe closed-loop dynamics, regardless of the rate of change of the operating points. Simulations for constant lateral acceleration demands show good tracking with fast response time. The second contribution is to interpret pseudolinearization as the restriction of feedback linearization[14] to the set of equilibria, and the third is to perform a successful pseudolinearising design for a QLPV system.

Parametric[15,16] and H_∞ (Ref. 17) stability margins for uncertainty in the controller parameters and aerodynamic derivatives are analyzed using Kharitonov's approach. The analysis shows that the design is fairly robust with respect to both kinds of uncertainty. The fourth contribution is to perform an effective robustness analysis, despite the involved parametric dependencies.

This paper is organized as follows. Section II presents the missile model, a classification of dynamics models with emphasis on QLPV systems, and input–output pseudolinearization After this background, Sec. III describes the auto-pilot design and the results of simulations, and in Sec. IV robust stability ana-lysis of the closed-loop system is considered. Conclusions follow in Sec. V.

II. Preliminaries

A. Missile Model

Missile autopilots are usually designed using linear models of nonlinear equations of motion and aerodynamic forces and moments.[15,18] The objective of this paper is robust design of a sideslip (yaw) velocity autopilot for a nonlinear missile model. This model describes a reasonably realistic airframe of a tail-controlled tactical missile in the cruciform fin configuration (see Fig. 1). The aerodynamic parameters in this model are derived from wind-tunnel measurements.[10]

The starting point for mathematical description of the missile is the following nonlinear model[10,19] of the horizontal motion (on the x–y plane in Fig. 1):

$$\begin{aligned}\dot{v} &= y_v(M,\lambda,\sigma)v - Ur + y_\zeta(M,\lambda,\sigma)\zeta \\ &= \tfrac{1}{2}m^{-1}\rho V_0 S\left(C_{y_v}v + V_0 C_{y_\zeta}\zeta\right) - Ur \\ \dot{r} &= n_v(M,\lambda,\sigma)v + n_r(M,\lambda,\sigma)r + n_\zeta(M,\lambda,\sigma)\zeta \\ &= \tfrac{1}{2}I_z^{-1}\rho V_0 S d\left(\tfrac{1}{2}dC_{n_r}r + C_{n_v}v + V_0 C_{n_\zeta}\zeta\right) \end{aligned} \quad (1)$$

where the variables are defined in Fig. 1. Here, v is the sideslip velocity; r is the body rate; ζ the rudder fin deflections; y_v and y_ζ semi-nondimensional force derivatives due to lateral and fin angle; and n_v, n_ζ, and n_r semi-nondimensional moment derivatives due to sideslip velocity, fin angle, and body rate. U is the longitudinal velocity. Furthermore, $m = 125$ kg is the missile mass, $\rho = \rho_0 - 0.094h$ air density ($\rho_0 = 1.23\ \mathrm{kg\,m^{-3}}$ is the sea level air density and h the missile altitude in km), V_0 the total velocity in $\mathrm{m\,s^{-1}}$, $S = \pi d^2/4 = 0.0314\ \mathrm{m^2}$ the reference area ($d = 0.2$ m is the reference diameter), and $I_z = 67.5\ \mathrm{kg\,m^2}$ is the lateral inertia. For the coefficients C_{y_v}, C_{y_ζ}, C_{n_r}, C_{n_v}, and C_{n_ζ} only discrete data points are available, obtained from wind-tunnel experiments. An interpolation formula for the Mach number $M \in [0.6, 6.0]$, roll angle $\lambda \in [4.5, 45\ \mathrm{deg}]$ and total incidence $\sigma \in [3, 30\ \mathrm{deg}]$ has been derived with the results summarized in Table 1.

Table 1 Coefficients in nonlinear model (1)

Coefficient	Coefficient name	Interpolated formula
C_{y_v}	Sideslip normal force	$0.5[(-25 + M - 60\lvert\sigma\rvert) \times (1 + \cos 4\lambda) + (-26 + 1.5M - 30\lvert\sigma\rvert)(1 - \cos 4\lambda)]$
C_{y_ζ}	Fin normal force	$10 + 0.5[(-1.6M + 2\lvert\sigma\rvert) \times (1 + \cos 4\lambda) + (-1.4M + 1.5\lvert\sigma\rvert)(1 - \cos 4\lambda)]$
C_{n_r}	Damping moment	$-500 - 30M + 200\lvert\sigma\rvert$
C_{n_v}	Sideslip moment	$s_m C_{y_v}$, where: $s_m = d^{-1}[1.3 + 0.1M + 0.2(1 + \cos 4\lambda)\lvert\sigma\rvert + 0.3(1 - \cos 4\lambda)\lvert\sigma\rvert - (13 + m/500)]$
C_{n_ζ}	Control moment	$s_f C_{y_\zeta}$, where: $s_f = d^{-1}[2.6 - (1.3 + m/500)]$

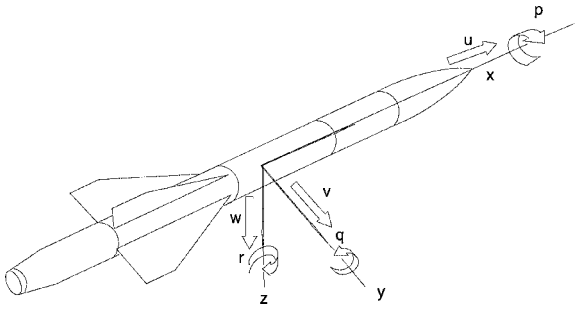

Fig. 1 Airframe axes.

The total velocity vector $\boldsymbol{V}_0$ is the sum of the longitudinal velocity vector $\boldsymbol{U}$ and the sideslip velocity vector $\boldsymbol{v}$, that is, $\boldsymbol{V}_0 = \boldsymbol{U} + \boldsymbol{v}$, with all three vectors lying on the x–y plane (see Fig. 1). We assume that $U \gg v$, so that the total incidence σ, or the angle between $\boldsymbol{U}$ and $\boldsymbol{V}_0$, can be taken as $\sigma = v/V_0$, as $\sin\sigma \approx \sigma$ for small σ. Thus, we have $\sigma = v/V_0 = v/\sqrt{(v^2 + U^2)}$, so that the total incidence is a nonlinear function of the sideslip velocity and longitudinal velocity, $\sigma = \sigma(v, U)$.

The Mach number is obviously defined as $M = V_0/a$, where a is the speed of sound. Because $V_0 = \sqrt{(v^2 + U^2)}$, the Mach number is also a nonlinear function of the sideslip velocity and longitudinal velocity, $M = M(v, U)$.

It follows from the preceding discussion that all coefficients in Table 1 can be in-terpreted as nonlinear functions of three variables: sideslip velocity v, longitudinal velocity U, and roll angle λ.

For an equilibrium (v_0, r_0, ζ_0) it is possible to derive from Eq. (1) a linear model in incremental variables, $\bar{v} \triangleq v - v_0$, $\bar{r} \triangleq r - r_0$, and $\bar{\zeta} \triangleq \zeta - \zeta_0$. In particular, for the straight, level flight (with gravity influence neglected), we have $(v_0, r_0, \zeta_0) = (0, 0, 0)$, so that the incremental and absolute variables are numerically identical, although conceptually different.

B. Taxonomy of Models

Mathematical representation of nonlinear missile dynamics aims at deriving models that adequately capture missile behaviour and are

practical for systematic control design. A taxonomy of dynamics models is presented in the following diagram, which should be viewed in conjunction with Eq. (1) and Table 1 of Sec. II.A.

The diagram shows the dynamics of missile models and their relationships, where $x = x(t)$ is the state, $u = u(t)$ the input, and $\theta = \theta(t)$ external parameters (variables different from x and u).

The lower left corner of the diagram is the LTI model:

$$\dot{x} = Ax + Bu, \qquad y = Cx \tag{2}$$

where $\boldsymbol{u} = u(t) \in \mathbb{R}^m$ is the vector of inputs, $\boldsymbol{x} = x(t) \in \mathbb{R}^n$ is the vector of states and $\boldsymbol{y} = y(t) \in \mathbb{R}^q$ is the vector of outputs. Finally, A, B, and C are matrices with constant real entries, $A \in \mathbb{R}^{n \times n}$, $B \in \mathbb{R}^{n \times m}$, and $C \in \mathbb{R}^{n \times q}$. This familiar model arises from Taylor linearization about a single flight condition and allows linear controller design, but has limited applicability for the whole flight envelope.

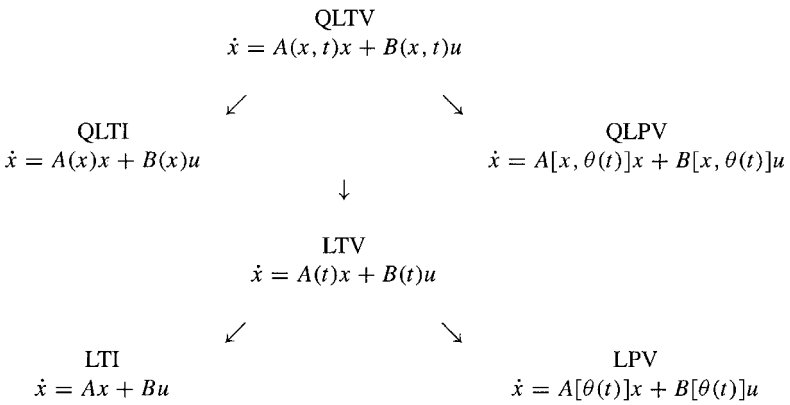

Traditionally, satisfactory performance across the flight envelope can be attained by gain scheduling local autopilot controllers to yield a global controller. The global controller is a collection of LTI controllers designed for the corresponding family of LTI models obtained via Taylor linearizations about equilibria. An LTI controller of the collection is switched on when the current operating point of the flight envelope is in the vicinity of the relevant equilibrium. This switching schedule is determined by the scheduling variables, which are external in the sense that they are different from state x and input u. A precise mathematical description of the resulting control system has recently been achieved with LPV models, appearing in the lower right corner of the preceding diagram:

$$\dot{x} = A[\theta(t)]x + B[\theta(t)]u, \qquad y = C[\theta(t)]x \tag{3}$$

The entries of matrices A, B, and C are no longer constant as in the LTI model (2), but are time varying, making LPV models a special case of linear time-varying LTV models, as symbolized in the diagram. The variation over time is determined by parameters θ, which represent a generalization of scheduling variables. Gain scheduling requires scheduling on a slow variable, which means that changes in θ should be much slower than changes in x and u. This requirement (violated for a rapidly maneuvering missile) is absent in the LPV model and, hence, it is a generalization of gain scheduling. This motivates recent interest in the LPV approach to autopilot design, as it promises to preserve the transparency of linear controller design while reflecting the rapidly changing missile dynamics.

However, the LPV model is still a collection of linear designs, and in each of those it is impossible to distinguish between real disturbances and normal manifestations of nonlinearity. Hence, any further improvement in performance and robustness can be achieved only by directly acknowledging missile nonlinearity, rather than treating it as nuisance in a linear model. Thus, the nonlinear dynamics must be explicitly incorporated into the mathematical description, but without undue generality. This is done in the upper part of the diagram in this section. The topmost model is quasi-linear time-varying (QLTV), which in the context of Eq. (1) and Table 1 of Sec. II.A is the most general framework we need:

$$\dot{x} = A(x,t)x + B(x,t)u, \qquad y = C(x,t)x \tag{4}$$

The most important novelty in the QLTV model over the models in the lower part of the diagram in this section is that it is nonlinear because matrices A, B, and C depend on state x. Note also that Eq. (4) is time-varying (A, B, and C depend on time t, as well).

Obviously, the LTV model is a special case of the QLTV model, but more important are the two nonlinear special cases, as illustrated in the diagram in this section. The top left one is the quasi-linear time-invariant (QLTI) model, obtained from Eq. (4) by simply dropping the explicit dependence on time t. The top right representation, the QLPV model, is the most relevant one here:

$$\dot{x} = A[x,\theta(t)]x + B[x,\theta(t)]u, \qquad y = C[x,\theta(t)]x \tag{5}$$

Mathematical description (5) is the focus of this paper, because close examination of Eq. (1) and Table 1 of Sec. II.A reveals that with $x \triangleq (v \;\; r)'$, $u \triangleq \zeta$, and $\theta \triangleq (U \;\; \lambda)'$, Eq. (1) is of the form of Eq. (5). This is pursued further in Sec. III.

C. Input–Output Pseudolinearization

Consider the nonlinear system with m inputs and q outputs:

$$\dot{x} = f(x,u), \qquad y = h(x) \tag{6}$$

where $f: \mathcal{X} \times \mathcal{U} \to \mathbb{R}^n$ and $h: \mathcal{X} \to \mathbb{R}^q$ are smooth and $\mathcal{X} \subset \mathbb{R}^n$ and $\mathcal{U} \subset \mathbb{R}^m$ are open sets. The set of equilibria of Eq. (6) is assumed to depend on parameters $p \in P \subset \mathbb{R}^\rho$, P open, and is denoted as

$$\mathfrak{E}(p) = \{[x_0(p), u_0(p)] \mid f[x_0(p), u_0(p)] = 0\} \tag{7}$$

where $x_0: P \to \mathcal{X}$ and $u_0: P \to \mathcal{U}$ are at least differentiable. Note that parameters p, unlike θ in the diagram of Sec. II.B, need not be external, that is, p may depend on x and/or u. In particular, p may depend on both state x and external parameters θ, which is used in Sec. III.

Let $\bar{x}(p) \triangleq x - x_0(p)$, $\bar{u}(p) \triangleq u - u_0(p)$, and $\bar{y}(p) \triangleq h(x) - h[x_0(p)]$ be the incremental variables arising from Taylor linearization of the open-loop system (6) at an equilibrium from $\mathfrak{E}(p)$. Setting $A(p) \triangleq \partial f/\partial x|_{[x_0(p),u_0(p)]}$, $B(p) \triangleq \partial f/\partial u|_{[x_0(p),u_0(p)]}$ and $C(p) \triangleq \partial h/\partial x|_{[x_0(p),u_0(p)]}$, the corresponding linearized system is

$$\dot{\bar{x}}(p) = A(p)\bar{x}(p) + B(p)\bar{u}(p), \qquad \bar{y}(p) = C(p)\bar{x}(p) \tag{8}$$

with the additional assumption that Eq. (8) is completely controllable and observable and has relative degree r for all points from $\mathfrak{E}(p)$ and all $p \in P$.

The problem of input–output pseudolinearization[11–13] is to find for system (6) the restriction of a state transformation $z = \Phi(x)$ to $\mathfrak{E}(p)$ and the restriction of a feedback law $u = k(x, v)$ (with v to be determined as a function of z and reference signal) to $\mathfrak{E}(p)$, so that Taylor linearization of the resulting closed-loop system is independent of the choice of equilibrium from $\mathfrak{E}(p)$ and parameter p from P. Note that, unlike for feedback linearization,[14] we are not looking for a global transformation $z = \Phi(x)$ and a global feedback law $u = k(x, v)$. We seek only their restrictions to the parameterized family of curves $\{\mathfrak{E}(p)\}_{p\in P}$, so that we need not find the whole of Φ and the whole of k. This simplifies the design considerably, but the resulting control law will be applicable only in the immediate neighborhood of $\{\mathfrak{E}(p)\}_{p\in P}$, not the whole $\mathcal{X}\times\mathcal{U}$. However, Taylor linearization of the resulting closed-loop system will be independent of p and, thus, of all equilibria of $\{\mathfrak{E}(p)\}$. In this way, if the operating points are in the vicinity of the equilibria, then one and only one linear model will describe closed-loop dynamics, regardless of the rate of change of the operating points. Note that the design cannot guarantee anything beyond the immediate neighborhood of $\{\mathfrak{E}(p)\}_{p\in P}$.

For a single-input/single-output (SISO) system (8) the restriction of $z = \Phi(x)$ and $u = k(x, v)$ to $\{\mathfrak{E}(p)\}_{p\in P}$ should give the following Taylor linearization in the (z, v) space {here, $\bar{z} \triangleq z - \Phi[x_0(p)]$ and $\bar{v} \triangleq v - v_0(p)$ with $u_0(p) = k[x_0(p), v_0(p)]$}:

$$\begin{aligned}
\dot{\bar{z}}_1 &= \bar{z}_2\\
&\vdots\\
\dot{\bar{z}}_{r-1} &= \bar{z}_r\\
\dot{\bar{z}}_r &= \bar{v}\\
\dot{\bar{z}}_{r+1} &= \boldsymbol{a}_{r+1}^T[x_0(p), u_0(p)]\bar{z}\\
&\vdots\\
\dot{\bar{z}}_n &= \boldsymbol{a}_n^T[x_0(p), u_0(p)]\bar{z}\\
\bar{y} &= \bar{z}_1
\end{aligned} \tag{9}$$

where only the n-dimensional vectors $\boldsymbol{a}_{r+1}, \ldots, \boldsymbol{a}_n$ still depend on equilibria from $\mathfrak{E}(p)$ and parameters from P. As the dynamics defined by $\boldsymbol{a}_{r+1}, \ldots, \boldsymbol{a}_n$ are unobservable (so must be stable), from the input–output viewpoint system (9) is linear of order r and remains the same for all current values of x_0, u_0, and p. This should be contrasted with Taylor linearization (8) of the open-loop system (6).

Input–output pseudolinearization may be interpreted as the restriction of feedback linearization[14] to the parameterized family of sets of equilibria $\{\mathfrak{E}(p)\}_{p\in P}$. The focus is on a small portion of the p parameterized (x, u) space, that is, on linearization along the parameterized family of curves $\{\mathfrak{E}(p)\}_{p\in P}$. Thus, it suffices to investigate the tangents $\partial\Phi/\partial x \triangleq T$ of Φ and $\partial k/\partial x \triangleq F$, and $\partial k/\partial v \triangleq G$ of k along $\{\mathfrak{E}(p)\}_{p\in P}$, rather than global properties of Φ and k. In particular[12,13] it is required that $T[x_0(p)]$ is invertible for all $p \in P$, and that feedback law $u = k(x, v)$ is smooth and satisfies $u_0(p) = k[x_0(p), v_0(p)]$, and that $G[x_0(p), v_0(p)]$ is invertible for all $p \in P$. The two conditions on k were implicitly used in the parenthetical statement preceeding Eq. (9), but explicit knowledge of k, or Φ, is not necessary even there, as $v_0(p)$, and $z_0(p)$, is never explicitly needed. Essentially, this is because the starting point of the design is Eq. (8), which is then transformed into Eq. (9). The formula for the tangent of transformation Φ along $\{\mathfrak{E}(p)\}_{p\in P}$ is[12,13]:

$$\bar{z} = T(p)\bar{x} \tag{10}$$

$$T(p) = \begin{bmatrix} C(p)\\ \vdots\\ C(p)A^{r-1}(p)\\ T_{r+1}(p)\\ \vdots\\ T_n(p) \end{bmatrix} \tag{11}$$

where rows T_i, $i = r+1, \ldots, n$ can be obtained from

$$\begin{bmatrix} T_{r+1}(p)\\ \vdots\\ T_n(p) \end{bmatrix} B(p) = 0 \tag{12}$$

which is a system of $n - r$ linear equations in $(n - r)n$ unknowns. Note that matrix T can be ill conditioned if the eigenvalues of A differ by orders of magnitude, which is a general weakness of all approaches based on state transformation. However, if it is possible to choose convenient p, this problem may be partially alleviated.

For the tangent of feedback law k along $\{\mathfrak{E}(p)\}_{p\in P}$ the formula is[12,13]:

$$\bar{u} = F(p)\bar{x} + G(p)\bar{v} \tag{13}$$

where

$$F(p) = -[C(p)A^{r-1}(p)B(p)]^{-1}C(p)A^r(p) \tag{14}$$

$$G(p) = [C(p)A^{r-1}(p)B(p)]^{-1} \tag{15}$$

Formulae (10–15) transform a SISO, Eq. (8), into Eq. (9). Design of a stabilizing control law (13) is complete when $\bar{v} = K_1\bar{z}_1 + \cdots + K_r\bar{z}_r$, where K_i, $i = 1, \ldots, r$ are constants. If the desired output $\bar{y}_d$ is nonzero, then the tracking error is $\bar{e} \triangleq \bar{y}_d - \bar{y} = \bar{y}_d - \bar{z}_1$ with its derivatives $\bar{e}^{(i)} = \bar{y}_d^{(i)} - \bar{z}_{i+1}$, $i = 1, \ldots, r-1$. Hence, the tracking control law will be $\bar{v} = K_1\bar{e} + \cdots + K_r\bar{e}^{(r-1)}$. Putting $\bar{z} = T(p)\bar{x}$ and $\bar{v}$ in Eq. (13) gives the feedback law in terms of $\bar{x}$, so that transformation T can be viewed as an auxiliary tool for designing the feedback control law (13). Thus-derived law (13) should be substituted in Eq. (8).

Geometrically, $\{\mathfrak{E}(p)\}_{p\in P}$ are general curves in the $(n + m)$ dimensional (x, u) space. They are projections of the corresponding $(n + m + n)$ dimensional curves from the $[x, u, f(x, u)]$ space, where f is the right-hand side of Eq. (6). Taylor linearizations in the $[x, u, f(x, u)]$ space at different points of curves $\{\mathfrak{E}(p)\}_{p\in P}$ involve straight lines of different tangents. Mapping Φ and feedback law k transform the general curves of the $[x, u, f(x, u)]$ space into a single straight line ℓ, whose projection on the (z, v) space is also a straight line, l. (A curve in the $[x, u, f(x, u)]$ space is fully determined by values of x and u alone. Thus, transformation of (x, u) into (z, v) by $x = \Phi^{-1}$, and, thus, $u = k[\Phi^{-1}(z), v]$, fully determines the new shape of the curve.) This line l is the image of curves $\{\mathfrak{E}(p)\}_{p\in P}$ in the (z, v) space under Φ and k. Taylor linearization along l gives one tangent for all points of $\{\mathfrak{E}(p)\}_{p\in P}$, namely the tangent of ℓ.

III. Design of Sideslip Velocity Autopilot

As explained in Sec. II.A, the Mach number M and the incidence σ are functions of v and U, so that the missile model given by Eq. (1) and Table 1 can be represented as

$$\begin{aligned}
\dot{v} &= y_v(v, U, \lambda)v - Ur + y_\zeta(v, U, \lambda)\zeta\\
\dot{r} &= n_v(v, U, \lambda)v + n_r(v, U, \lambda)r + n_\zeta(v, U, \lambda)\zeta
\end{aligned} \tag{16}$$

Recall from Sec. II.A. that for the straight, level flight (with gravity influence neglected) the incremental and absolute variables are numerically identical. Therefore, setting

$$\bar{x} \triangleq \begin{bmatrix} v\\ r \end{bmatrix}, \qquad p \triangleq \begin{bmatrix} v\\ U\\ \lambda \end{bmatrix}, \qquad \bar{u} \triangleq \zeta, \qquad \bar{y} \triangleq v \tag{17}$$

Eqs. (16) lead to the following description:

$$\dot{\bar{x}} = A(p)\bar{x} + B(p)\bar{u}, \qquad \bar{y} = C\bar{x} \tag{18}$$

where

$$A(p) = \begin{bmatrix} y_v(p) & -p_2\\ n_v(p) & n_r(p) \end{bmatrix}, \qquad B(p) = \begin{bmatrix} y_\zeta(p)\\ n_\zeta(p) \end{bmatrix}$$

$$C = [1 \quad 0] \tag{19}$$

Thus, representation (16) can be seen as the QLPV model (cf. diagram, Sec. II.B), because p in Eq. (17) comprises both a state and external parameters (longitudinal velocity U and roll angle λ), so that matrices (19) depend both on $\bar{x}$ and θ. On the other hand, Eq. (18) is also of the form of Eq. (8), which allows the use of pseudolinearization

Although we use incremental sideslip velocity v as output [see Eq. (17)], the demand usually is given in terms of lateral acceleration a_v. Because $a_v = \dot{v} + Ur$, we can use Eq. (16) to obtain $a_v = y_v v + y_\zeta \zeta$. The term $y_\zeta \zeta$ will be small because it represents the lateral force developed by the tail fin. As the moment arm of the tail fin is usually much greater than the missile static margin, the tail force $y_\zeta \zeta$ is much smaller than the wing and body lateral force $y_v v$, and so we can use the approximation $a_v \approx y_v v$, which is a static nonlinear relationship between lateral acceleration and sideslip velocity. This can then be used to translate approximately the a_v demand into v demand.

Our design of the sideslip velocity autopilot takes the second-order ($n = 2$) model (18) and (19) as the starting point. Noting that the relative degree r is 2, we then use formulae (10–15). Because in our case $r = n$, we have no need for Eq. (12), so that

$$T(p) = \begin{bmatrix} C \\ CA(p) \end{bmatrix} = \begin{bmatrix} 1 & 0 \\ y_v(p) & -p_2 \end{bmatrix} \tag{20}$$

The control law will be

$$\bar{u} = F(p)\bar{x} + G(p)\bar{w} \tag{21}$$

where $\bar{w}$ is the fictitious input still to be determined in terms of $\bar{x}$ and the reference signal. Matrix F is

$$F(p) = -[CA(p)B(p)]^{-1}CA^2 = [1/a(p)][-b_1(p) \quad -b_2(p)] \tag{22}$$

and scalar G

$$G(p) = [CA(p)B(p)]^{-1} = 1/a(p) \tag{23}$$

where

$$b_1(p) = y_v^2(p) - n_v(p)p_2, \qquad b_2(p) = -y_v(p)p_2 - n_r(p)p_2$$
$$a(p) = y_v(p)y_\zeta(p) - n_\zeta(p)p_2 \tag{24}$$

When we substitute Eqs. (22) and (23) into Eq. (21), the resulting pseudolinearizing control is

$$\zeta = [1/a(p)][-b_1(p)v - b_2(p)r + \bar{w}] \tag{25}$$

which still requires defining $\bar{w}$ to ensure tracking. Let $\bar{e} \triangleq v_d - v$ be the sideslip velocity error, where v_d is the sideslip velocity demand derived from piecewise constant lateral acceleration demand. Then the final form of the control law is

$$\zeta = [1/a(p)][-b_1(p)v - b_2(p)r + K_1\bar{e} + K_2\dot{\bar{e}}] \tag{26}$$

The constants K_1 and K_2 in Eq. (26) are chosen as $K_1 = \omega_n^2$ and $K_2 = 2\xi\omega_n$, where $\omega_n = 70$ rad/s and $\xi = 0.7$, so that the error equation is $\ddot{\bar{e}} + 2\xi\omega_n\dot{\bar{e}} + \omega_n^2\bar{e} = 0$. This should give a 3–4 times faster response than in the open loop.

In practice, the acceleration demand will not be constant, and $\dot{\bar{e}}$ will be generated by $\dot{\bar{e}} = -\dot{v} = -y_v(p) + p_2 r$ with $\dot{v}_d = 0$. This will not affect the stability of the closed-loop system, but will slightly degrade the dynamic performance. This slight degradation is acceptable, and it also means that the demand does not need differentiation.

Simulation results for 300 m/s^2 constant demands in lateral acceleration are shown in Fig. 2. The steady-state error in lateral acceleration is about 1%.

Recall that the sideslip velocity demand was derived approximately from the original lateral acceleration demand. The static approximation neglected the fin force term $y_\zeta \zeta$. The effect of this term is evident in the nonminimum phase characteristic in lateral acceleration a_v. Note also that the initial fin angle $\zeta < 0$. On the other hand, in Fig. 2 the initial undershoot of -36.7 m/s^2 for a_v is not easily discernible due to the axes scaling, but its presence is also validated by $\zeta < 0$. These phenomena occur because the fin force dominates in the initial acceleration response. This is quickly overcome by the sideslip force as incidence builds up. The steady-state error represents the fin force contribution that was neglected in the analysis.

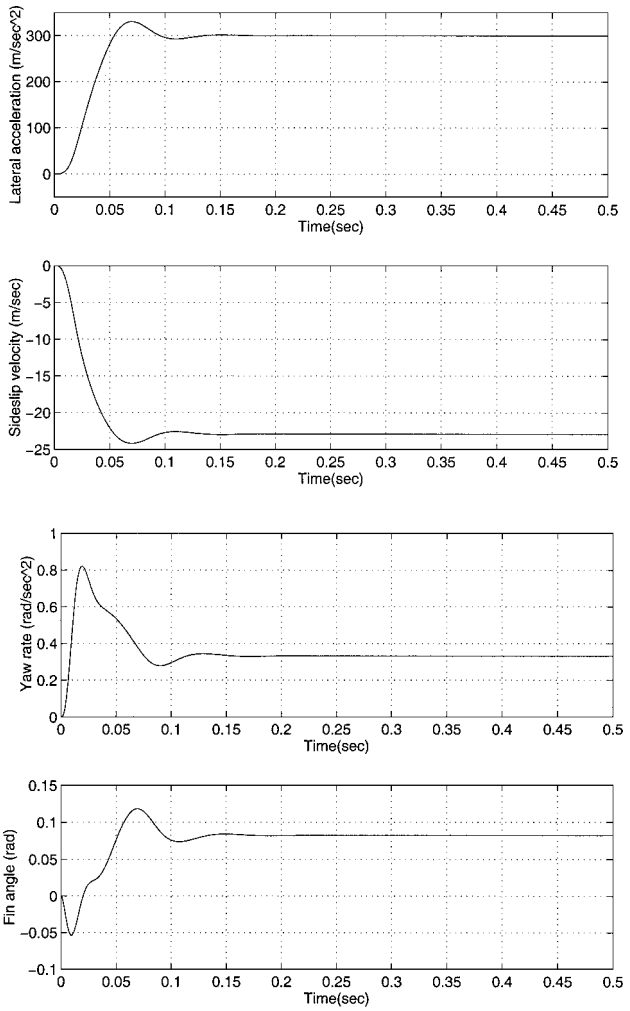

Fig. 2 Simulation for constant lateral acceleration demand of 300 ms^{-2}.

IV. Robust Stability Analysis

Unstructured uncertainties represent the effects of high-frequency unmodeled dynamics, nonlinearities, and errors due to linearization, etc., and are usually modelled as a ball of norm-bounded operators. It has been shown[20] that certain types of robust performance problems, specified in terms of norms, can be posed as robust stability problems under unstructured perturbations. By structured uncertainty[15,16] we mean parametric uncertainty representing lack of precise knowledge of the actual system parameters. In this section we analyze stability of the autopilot designed in Sec. III with uncertainties of mixed type[21] with the objective of quantifying, as nonconservatively as possible, the sizes of perturbations that can be tolerated by the closed-loop system. We attempt to do this by considering unstructured perturbations acting around an interval system.

A. Nominal Model

The sideslip velocity autopilot closed-loop characteristic equation can be obtained by substituting control law (26) into Eq. (16). This yields

$$\dot{v} = y_v(p)v - p_2 r + [y_\zeta/a(p)][-b_1(p)v - b_2(p)r + K_1\bar{e} + K_2\dot{\bar{e}}]$$
$$\dot{r} = n_v(p)v + n_r(p)r$$
$$+ [n_\zeta/a(p)][-b_1(p)v - b_2(p)r + K_1\bar{e} + K_2\dot{\bar{e}}] \tag{27}$$

When we assume that the derivative $\dot{v}_d$ of the sideslip velocity demand is zero, we have $\dot{\bar{e}} = -\dot{v}$. Then the closed-loop equations (27) can be rewritten as

$$E(p)\dot{\bar{x}} = A_c(p)\bar{x} + B_c(p)v_d, \qquad \bar{y} = C\bar{x} \tag{28}$$

with $\bar{x}$, $\bar{y}$, and p as in Eq. (17) and matrices E, A_c, B_c, and C given as

$$E(p) = \begin{bmatrix} a(p) + y_\zeta(p)K_2 & 0 \\ n_\zeta(p)K_2 & a(p) \end{bmatrix}$$

$$A_c(p) =$$

$$\begin{bmatrix} y_v(p)a(p) - y_\zeta(p)b_1(p) - y_\zeta(p)K_1 & -p_2 a(p) - y_\zeta(p)b_2(p) \\ n_v(p)a(p) - n_\zeta(p)b_1(p) - n_\zeta(p)K_1 & n_r(p)a(p) - n_\zeta(p)b_2(p) \end{bmatrix}$$

$$B_c(p) = \begin{bmatrix} y_\zeta(p)K_1 \\ n_\zeta(p)K_1 \end{bmatrix}, \qquad C = [1 \quad 0] \tag{29}$$

For the purposes of robust stability analysis, we assume that Eqs. (28) and (29) represent an uncertain LTI model, whose uncertainty is caused by variations in p (recall that p_1 is a state). Then the nominal transfer function from v_d to v is

$$G(s) = C[sE - A_c]^{-1}B_c = n(s)/d(s) \tag{30}$$

where

$$n(s) = K_1 y_\zeta s - K_1(n_r y_\zeta + U n_\zeta)$$

$$\begin{aligned} d(s) = {} & (a + y_\zeta K_2)s^2 - [a(n_r + y_v) - n_\zeta b_2 - y_\zeta b_1 \\ & + (y_\zeta n_r + U n_\zeta)K_2 - y_\zeta K_1]s + [a(y_v n_r + U n_v) \\ & + (y_\zeta n_v - y_v n_\zeta)b_2 - (y_\zeta n_r + U n_\zeta)b_1 - (y_\zeta n_r + U n_\zeta)K_1] \end{aligned} \tag{31}$$

B. Worst-Case Parametric Stability Margin

In this section the stability margins associated with two kinds of parametric uncertainty, 1) varying controller parameters a, b_1, and b_2 and 2) varying aerodynamics parameters y_v, U, n_r, n_v, and n_ζ are analyzed. The problem can be simplified by making the same approximations that were used in the design process by neglecting the fin angle force y_ζ. Then the characteristic polynomial becomes

$$\begin{aligned} d(s) = {} & as^2 - [a(n_r + y_v) - n_\zeta b_2 + U n_\zeta K_2]s \\ & + [a(y_v n_r + U n_v) - y_v n_\zeta b_2 - U n_\zeta b_1 - U n_\zeta K_1] \end{aligned} \tag{32}$$

1. *Controller Stability Analysis*

To assess the robustness to controller parameters errors in a, b_1, and b_2, we first define their nominal values:

$$\hat{b}_1 = y_v^2 - n_v U, \qquad \hat{b}_2 = -y_v U - n_r U, \qquad \hat{a} = -n_\zeta U \tag{33}$$

When we assume an error model of the form

$$b_1 = \hat{b}_1 + \Delta b_1, \qquad b_2 = \hat{b}_2 + \Delta b_2, \qquad a = \hat{a} + \Delta a \tag{34}$$

the uncertainty in characteristic polynomial (32) is

$$\begin{aligned} d(s) = {} & (\hat{a} + \Delta a)s^2 + [\hat{a}K_2 - (n_r + y_v)\Delta a + n_\zeta \Delta b_2]s \\ & + [\hat{a}K_1 + (y_v n_r + n_v U)\Delta a - y_v n_\zeta \Delta b_2 + \hat{a}\Delta b_1] \end{aligned} \tag{35}$$

This equation is in the affine form[16]

$$d(s) = \delta_0(s) + \sum_{i=1}^{3} \delta_i(s) q_i \tag{36}$$

where q_i are relative errors (in percent)

$$q_1 \triangleq \Delta a/\hat{a}, \qquad q_2 \triangleq \Delta b_2/\hat{b}_2, \qquad q_3 \triangleq \Delta b_1/\hat{b}_1 \tag{37}$$

and $|q_i| \le s_i$ with s_i the range of parameter uncertainty in percent. From Eqs. (35–37)

$$\begin{aligned} \delta_0(s) &= \hat{a}\left[(1 + K_2)s^2 + K_1\right] \\ \delta_1(s) &= \hat{a}\left[s^2 - (n_r + y_v)s + (y_v n_r + n_v U)\right] \\ \delta_2(s) &= \hat{b}_2(n_\zeta s - y_v n_\zeta), \qquad \delta_3(s) = \hat{a}\hat{b}_1 \end{aligned} \tag{38}$$

Note that the frequency response lies within the image set, hence, a qualitative view on the uncertainty in time response can be obtained from the image plot. The convex hull of mapped vertices across a grid of frequencies is shown in Fig. 3. The zero exclusion condition[16]

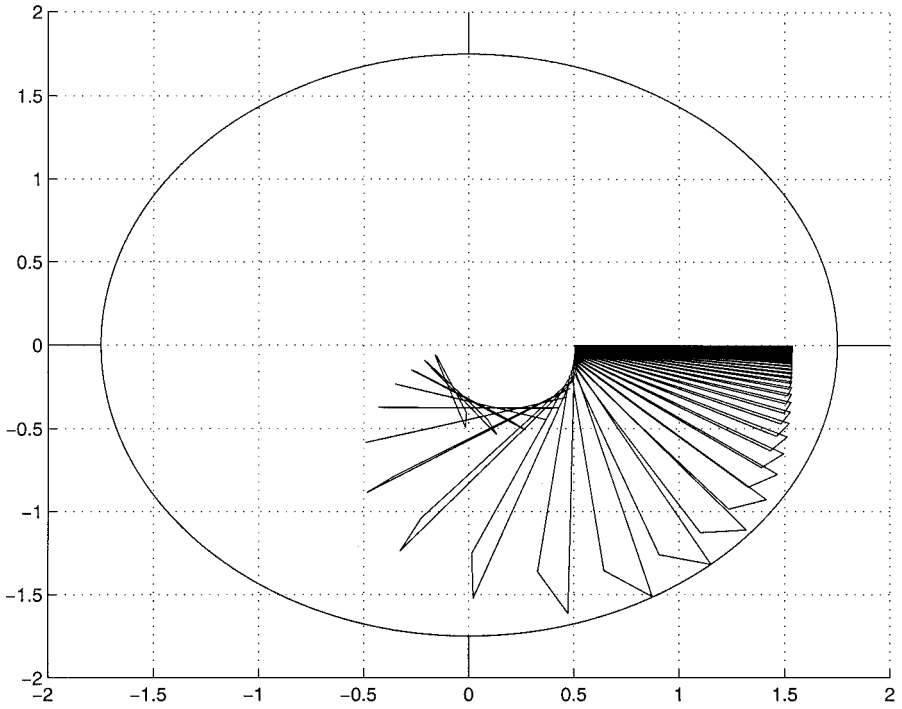

Fig. 3 Frequency template of G_K and H_∞ stability margin for variations in controller parameters.

is satisfied for parameter variation of 70% for a and b_2 and 100% for b_1. As expected, the greatest effect is changing the gain a. A smaller, but significant effect occurs when b_2 is inaccurate. This manifests itself in a loss of damping characterized by a vertical shift in the frequency response. The term b_1 has negligible effect on the robustness of the system.

2. Aerodynamic Derivatives Stability Analysis

The uncertainty in aerodynamic derivatives can also be studied using Kharitonov techniques. The approach used here assumes that the true values and the design values are in error. The error model is, thus,

$$y_v = \hat{y}_v + \Delta y_v, \qquad n_v = \hat{n}_v + \Delta n_v, \qquad n_r = \hat{n}_r + \Delta n_r$$
$$n_\zeta = \hat{n}_\zeta + \Delta n_\zeta, \qquad U = \hat{U} + \Delta U \tag{39}$$

The controller parameters then have the following form:

$$\hat{a} + \Delta a = -(\hat{U} + \Delta U)(\hat{n}_\zeta + \Delta n_\zeta)$$
$$\Delta a = -\hat{U}\Delta n_\zeta - \hat{n}_\zeta \Delta U - \Delta U \Delta n_\zeta$$
$$\hat{b}_1 + \Delta b_1 = (\hat{y}_v + \Delta y_v)^2 - (\hat{U} + \Delta U)(\hat{n}_v + \Delta n_v)$$
$$\Delta b_1 = 2\hat{y}_v \Delta y_v - \hat{n}_v \Delta U - \hat{U}\Delta n_v + \Delta y_v^2 - \Delta U \Delta n_v$$
$$\hat{b}_2 + \Delta b_2 = -(\hat{U} + \Delta U)(\hat{y}_v + \Delta y_v + \hat{n}_r + \Delta n_r)$$
$$\Delta b_2 = -(\hat{n}_r + \hat{y}_v)\Delta U - \hat{U}\Delta y_v - \hat{U}\Delta n_r - \Delta U \Delta y_v - \Delta U \Delta n_r \tag{40}$$

The characteristic polynomial takes the multiaffine form

$$d(s) = \delta_0(s) + \sum_{i=1}^{6} \delta_i(s) q_i + \sum_{i,j=1}^{6} \delta_{i,j}(s) q_i q_j + \sum_{i,j,k=1}^{6} \delta_{i,j,k}(s) q_i q_j q_k \tag{41}$$

where

$$q_1 \triangleq \frac{\Delta y_v}{\hat{y}_v}, \qquad q_2 \triangleq \frac{\Delta U}{\hat{U}}, \qquad q_3 \triangleq \frac{\Delta n_v}{\hat{n}_v}$$
$$q_4 \triangleq \frac{\Delta n_r}{\hat{n}_r}, \qquad q_5 \triangleq \frac{\Delta n_\zeta}{\hat{n}_\zeta}, \qquad q_6 \triangleq \frac{\Delta (y_v)^2}{(\hat{y}_v)^2} \tag{42}$$

and

$$\delta_0(s) = s^2\hat{a} + s\left[n_\zeta y_v^2 - \hat{a}(n_r + y_v - n_v - K_2)\right] + K_1\hat{a}$$
$$\delta_1(s) = s n_\zeta (U + 2y_v)\hat{y}_v$$
$$\delta_2(s) = \left[-s^2 + s(-K_2 + n_r + y_v - n_v) - K_1\right] n_\zeta \hat{U}$$
$$\delta_3(s) = s\hat{a}\hat{n}_v, \qquad \delta_4(s) = -s\hat{a}\hat{n}_r$$
$$\delta_5(s) = \left[-s^2 U + s\left(U n_r + U y_v - n_v U - K_2 U + y_v^2\right) - K_1 U\right]\hat{n}_\zeta$$
$$\delta_6(s) = s n_\zeta (\hat{y}_v)^2, \qquad \delta_{1,2}(s) = s n_\zeta \hat{y}_v \hat{U}$$
$$\delta_{1,5}(s) = s(U + 2y_v)\hat{y}_v \hat{n}_\zeta, \qquad \delta_{2,3}(s) = -s n_\zeta \hat{U}\hat{n}_v$$
$$\delta_{2,4}(s) = s n_\zeta \hat{U}\hat{n}_r$$
$$\delta_{2,5}(s) = \left[-s^2 + s(n_r + y_v - n_v - K_2) - K_1\right]\hat{U}\hat{n}_\zeta$$
$$\delta_{3,5}(s) = -sU\hat{n}_v\hat{n}_\zeta, \qquad \delta_{4,5}(s) = sU\hat{n}_r\hat{n}_\zeta$$
$$\delta_{5,6}(s) = s\hat{n}_\zeta(\hat{y}_v)^2, \qquad \delta_{1,2,5}(s) = s\hat{y}_v\hat{U}\hat{n}_\zeta$$
$$\delta_{2,3,5}(s) = -s\hat{U}\hat{n}_v\hat{n}_\zeta, \qquad \delta_{2,4,5}(s) = s\hat{U}\hat{n}_r\hat{n}_\zeta \tag{43}$$

The remaining δ are zero.

Note that characteristic polynomial (41) is multiaffine if the term $(\Delta y_v)^2$ is treated as an independent variable, unconnected with Δy_v. This clearly is not the case and will, therefore, give conservative results in the image set. This should, however, be insignificant because the uncertainty in b_1 was shown to have little effect on the robustness of the autopilot.

The convex hull of mapped vertices across a grid of frequencies is shown in Fig. 4. The aerodynamic derivative n_v has little influence on the performance and the robustness, as has y_v^2. Both can be varied by up to 100% without approaching instability. The U terms and the n_ζ terms represent the most sensitive parameters and have a similar effect on stability. Because these parameters will dominate the image set when all parameters vary together, a reduced variation of 20% is chosen for them. For the remaining aerodynamic derivatives, the zero exclusion condition is satisfied for parameter variation of 90%. It takes a long time to compute the image set for all of the parameters, as the vertex number and edge number increases as 2^n for n parameters. This is usually the reason why the convex

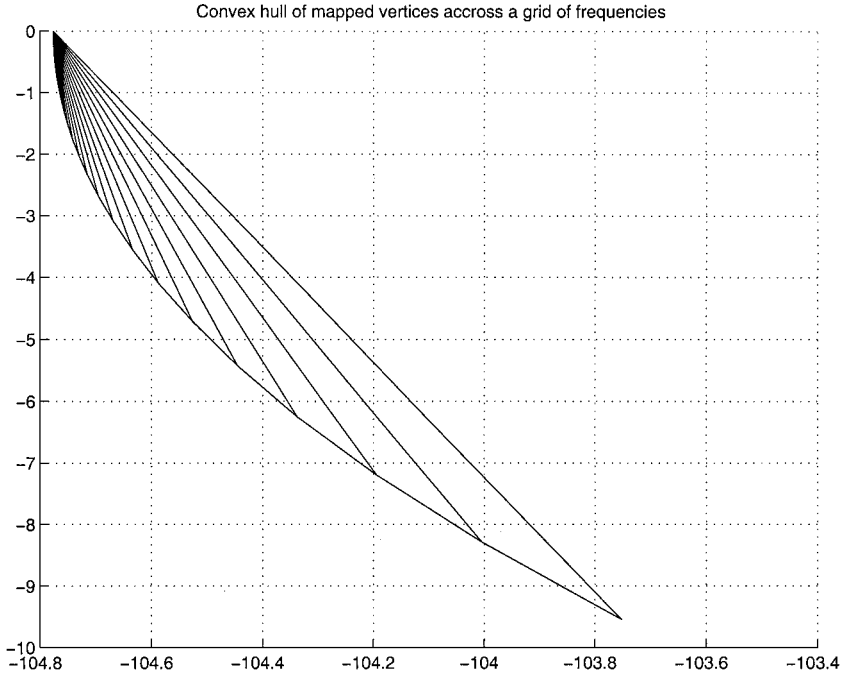

Fig. 4 Aerodynamic derivatives stability analysis using the mapping theorem.

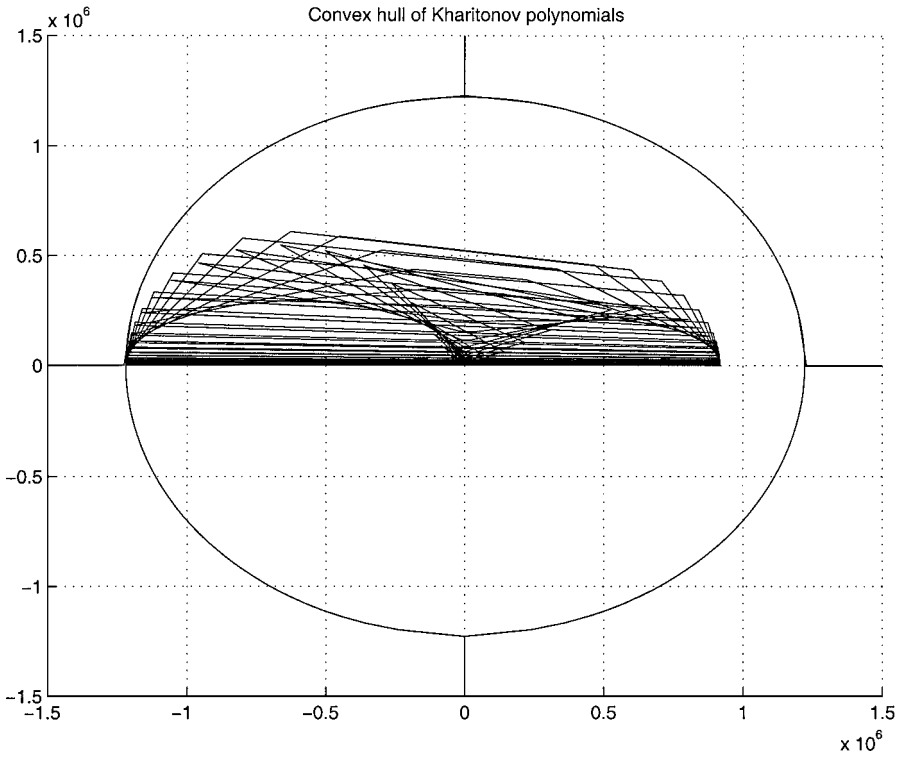

Fig. 5 Frequency template of G_K and H_∞ stability margin for variations in aerodynamic derivatives.

hull for Kharitonov polynomials is used instead of mapped vertices, even if the results are more conservative.

C. Worst-Case H_∞ Stability Margin

To compute the radius α of the ball of the maximum allowable unstructured perturbation that does not destroy closed-loop stability, it is sufficient to compute the maximum H_∞ norm of Kharitonov polynomials. This is stated at the following theorem (Theorem 9.2 on page 389 of Ref. 17).

Theorem 1: Let $G(s) = N(s)/D(s)$ be an uncertain closed-loop system and

$$G_K(s) = \left\{ \frac{K_N^i(s)}{K_D^j(s)} \,\middle|\, i, j \in \{1, 2, 3, 4\} \right\}$$

be the interval family of stable proper systems with $K_N^i(s)$ and $K_D^j(s)$ denoting the Kharitonov polynomials associated with $N(s)$ and $D(s)$, respectively. Then G is stable for all perturbations ΔG such that $\|\Delta G\|_\infty < \alpha$ if and only if

$$\alpha \leq 1 \Big/ \max_{G \in G_K} \|G\|_\infty$$

This is a significant reduction in computation because it replaces testing norms of an infinite family of functions with that of a finite set. To compute the worst-case H_∞ stability margin of our system, we need to plot the frequency template $G(j\omega)$.

Using the results of Sec. IV.B.1, we applied Theorem 1 to find from Fig. 3 the worst-case H_∞ stability margin, $\alpha = 057$, for variations in controller parameters.

It follows from Eq. (31) that the numerator of G is not affected by variations in controller parameters a, b_1, and b_2, so that family G_K has only four elements:

$$\|G_1\|_\infty = 0.5798, \qquad \|G_2\|_\infty = 0.5185$$

$$\|G_3\|_\infty = 1.5725, \qquad \|G_4\|_\infty = 1.7539$$

Therefore, the entire family of systems is stable under any unstructured feedback perturbation of H_∞ norm less than

$$\alpha = 1/1.7539 = 0.57$$

Then, using the results of Sec. IV.B.2, we applied Theorem 1 to find from Fig. 5 the worst-case H_∞ stability margin, $\alpha = 0.819 \times 10^{-6}$, for variations in aerodynamic derivatives.

By the use of Lemma 9.1 on page 389 in Ref. 17, it was found that the entire family of systems $G_K(s)$ is stable under any unstructured feedback perturbation of H_∞ norm less than

$$\alpha = 1 \Big/ \max_{G \in G_K} \|G\|_\infty = 0.82 \times 10^{-6}$$

For both controller parameters and aerodynamic derivatives the worst-case H_∞ stability margins found from Figs. 3 and 5 give the same results as the computation of the H_∞ norm at the Kharitonov vertices based on Lemma 9.1 on page 389 in Ref. 17.

V. Conclusions

It has been shown that a reasonably realistic missile model can be described as a QLPV system. This suggests that the QLTV dynamics description (of which QLPV is a special case) is not only relevant, but also offers the proper level of generality for nonlinear representation of missiles. The second conclusion is that QLPV models are amenable to input–output pseudolinearizing design, which results in a controller that depends both on the state and external parameters. The third conclusion is that the pseudolinearizing autopilot is free of the difficulties associated with gain scheduling because it consists of one controller only and scheduling is done automatically by feedback, which gives total independence of the operating point. However, the pseudolinearizing design is only valid (as gain scheduling is) in the vicinity of the equilibria and the state transformation matrix may be ill conditioned. The fourth conclusion is that an effective robustness analysis was possible by treating the closed-loop system as an uncertain LTI model. However, the Kharitonov approach employed led to rather tedious computations, and it would be nontrivial to extend it to missile models of higher order. Finally, the choice of output allowed having the relative degree equal to the order of the system, so that no unobservable dynamics were involved, which would have required their stability analysis and could have diminished closed-loop performance.

References

[1] Rugh, W. J., "Analytical Framework for Gain Scheduling," *IEEE Control Systems Magazine*, Vol. 11, No. 1, 1991, pp. 79–84.

[2]Kamen, E. W., and Khargonekar, P. P., "On the Control of Linear Systems Whose Coefficients are Functions of Parameters," *IEEE Transactions on Automatic Control*, Vol. 29, No. 1, 1984, pp. 25–33.

[3]Baumann, W. T., and Rugh, W. J., "Feedback Control of Nonlinear Systems by Extended Linearization," *IEEE Transactions on Automatic Control*, Vol. 31, No. 1, 1986, pp. 40–46.

[4]Wang, J., and Rugh, W. J., "Parameterized Linear Systems and Linearization Families for Nonlinear Systems," *IEEE Transactions on Circuits and Systems*, Vol. 34, No. 6, 1987, pp. 650–657.

[5]Shamma, J. S., and Athans, M., "Analysis of Gain Scheduled Control for Nonlinear Plants," *IEEE Transactions on Automatic Control*, Vol. 35, No. 8, 1990, pp. 898–907.

[6]Shamma, J. S., and Athans, M., "Guaranteed Properties of Gain Scheduled Control for Linear Parameter-Varying Plants," *Automatica*, Vol. 27, No. 3, 1991, pp. 559–564.

[7]Shamma, J. S., and Athans, M., "Gain Scheduling: Potential Hazards and Possible Remedies," *IEEE Control Systems Magazine*, Vol. 13, No. 3, 1992, pp. 101–107.

[8]Shahruz, S. M., and Behtash, S., "Design of Controllers for Linear Parameter Varying Systems by the Gain Scheduling Technique," *Journal of Mathematical Analysis and Applications*, Vol. 168, No. 1, 1992, pp. 195–217.

[9]Shamma, J. S., and Cloutier, J. R., "Gain-Scheduled Missile Autopilot Design Using LPV Transformations," *Journal of Guidance, Control and Dynamics*, Vol. 16, No. 2, 1993, pp. 256–263.

[10]Horton, M. P., "A Study of Autopilots for the Adaptive Control of Tactical Guided Missiles," M.S. Thesis, Dept. of Electrical Engineering, Univ. of Bath, England, U.K., Sept. 1992.

[11]Reboulet, C., and Champetier, C., "A New Method for Linearizing Nonlinear Systems: The Pseudolinearization," *International Journal of Control*, Vol. 40, No. 4, 1984, pp. 631–638.

[12]Lawrence, D. A., and Rugh, W. J., "Input–Output Pseudolinearization for Nonlinear Systems," *IEEE Transactions on Automatic Control*, Vol. 39, No. 11, 1994, pp. 2207–2218.

[13]Lawrence, D. A., "A Genereal Approach to Input–Output Pseudolinearization for Nonlinear Systems," *IEEE Transactions on Automatic Control*, Vol. 43, No. 10, 1998, pp. 1497–1501.

[14]Isidori, A., *Nonlinear Control Systems: An Introduction*, 2nd ed., Springer–Verlag, New York, 1989, pp. 137–172.

[15]Wise, K. A., "Comparison of Six Robustness Tests Evaluating Missile Autopilot Robustness to Uncertain Aerodynamics," *Journal of Guidance, Control, and Dynamics*, Vol. 15, No. 4, 1992, pp. 861–870.

[16]Barmish, B. R., *New Tools for Robustness of Linear Systems*, Macmillan, New York, 1994, pp. 237–253.

[17]Bhattacharyya, S. P., Chapellat, H., and Keel, L. H., *Robust Control, The Parametric Approach*, Prentice–Hall, Upper Saddle River, NJ, 1995, pp. 386–406.

[18]Horton, M. P., "Autopilots for Tactical Missiles: An Overview," *IMechE: Journal of Systems and Control Engineering*, Vol. 209, No. 12, 1995, pp. 127–139.

[19]Tsourdos, A., Blumel, A., and White, B. A., "Trajectory Control of a Nonlinear Homing Missile," *Proceedings of the 14th IFAC Symposium on Automatic Control in Aerospace*, Elsevier Sciences Ltd., Oxford, U.K., 1998, pp. 118–123.

[20]Daheleh, M., Tesi, A., and Vicino, A., "An Overview of Extremal Properties for Robust Control of Interval Plants," *Automatica*, Vol. 29, No. 3, 1993, pp. 707–721.

[21]Djaferis, T. E., *Robust Control Design—A Polynomial Approach*, Kluwer Academic, Norwell, MA, 1995, pp. 79–99.